

Thermodynamic Properties and Kinetic Parameters for Cyclic Ether Formation from Hydroperoxyalkyl Radicals

Catherina D. Wijaya, Raman Sumathi, and William H. Green, Jr.*

Department of Chemical Engineering, Massachusetts Institute of Technology, 77 Massachusetts Ave. Rm 66-270, Cambridge, Massachusetts 02139

Received: November 16, 2002; In Final Form: February 28, 2003

Rates and thermochemistry for the cyclization of various hydroperoxyalkyl radicals $\cdot\text{QOOH}$ with up to six carbons to form cyclic ethers plus OH are computed using complete-basis-set (CBS) and density-functional theory (DFT) methods. Effects of mono- and dialkyl substitution α to the OOH group and β to the radical center were also studied. Many quantum chemical methods have difficulty accurately predicting peroxide energetics and particular problems with the transition state calculations. The popular B3LYP method underestimates many barrier heights as well as O–O bond strengths by up to 8 kcal/mol. The related BH&HLYP method appears to give more accurate barrier heights predictions than B3LYP, but its thermochemistry is inaccurate and it overestimates the heats of reaction by up to 5 kcal/mol. For the transition states, there are subtle problems even with high-level CBS methods. But from the many calculations, a consistent picture emerges and is compared with the limited existing experimental data. Improved hydrogen-bond increment (HBI) values for β -hydroperoxyalkyl radicals and ring strain corrections (RSC) for cyclic ethers with 3-, 4-, and 5-membered rings are derived. Generalized rate estimation rules for the decomposition of alkyl-substituted $\cdot\text{QOOH}$ to form cyclic ethers are presented based on the observed Evans–Polanyi correlation between the computed barrier height and the reaction exothermicity. Issues that must be resolved before these results can be usefully applied in ignition and partial oxidation models are outlined.

I. Introduction

Recently a new type of engine called homogeneous charge compression ignition (HCCI) has been in the spotlight, due to its low NO_x and particular matter (PM) emissions and high efficiency.¹ These advantages come from lean and premixed combustion at relatively low temperatures. However, it has the drawback of high hydrocarbon and carbon monoxide emissions, and it is difficult to control the ignition timing and heat release rate during combustion. To overcome these problems, it is necessary to have an improved understanding of the oxidation chemistry^{2–6} of air/fuel mixtures at cool-flame temperatures.

Moderate temperature (500–1000 K) oxidation of hydrocarbon fuels is largely governed by the kinetics of chemically activated alkylperoxy intermediates (RO_2^*), which isomerize to hydroperoxyalkyl radicals ($\cdot\text{QOOH}$) in competition with dissociation to form alkyl radicals or alkenes. It is believed that a portion of the $\cdot\text{QOOH}$ reacts with O_2 to form three new radicals and that this is the main chain-branching reaction that controls the oxidation rate.^{7–10} However, the many reaction pathways and their corresponding rate parameters for the formation and disappearance of $\cdot\text{QOOH}$ (Figure 1) are not well established. Even the thermochemical parameters of some of these intermediates are doubtful. Thus here the decomposition of $\cdot\text{QOOH}$ to form cyclic ethers is examined theoretically.

Experimentally, the vapor-phase oxidation of C_6 – C_{16} hydrocarbons¹¹ yields 11–25 wt % heterocyclic oxygenates as products. From *n*-hexane, this cyclic ether fraction contained 59% oxolanes (five-membered rings, also known as THF), 35%

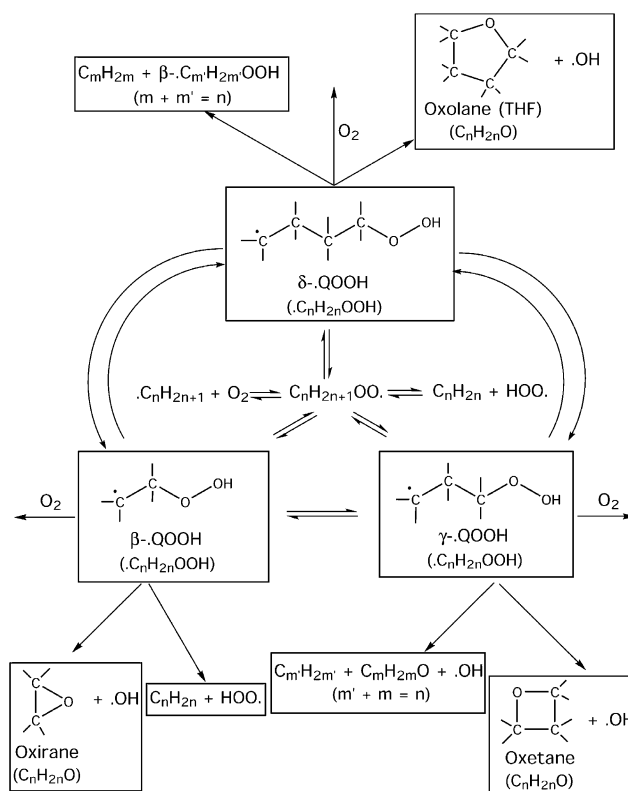


Figure 1. RO_2 reaction pathways important in low-temperature oxidation.

oxetanes (four-membered rings), and about 6% oxiranes (three-membered rings). From *n*-heptane, the cyclic ether fraction

* Corresponding author. Fax: 001(617)324-0066. E-mail: whgreen@mit.edu.

contained 68% oxolanes, 26% oxetanes, and 6% oxiranes. The moderate-temperature (580–600 K) oxidation of primary reference fuels *n*-heptane and isooctane (2,2,4-trimethylpentane) with air in a jet-stirred-flow reactor^{12,13} at pressures as high as 40 bar yielded, respectively, 10 and 60 mol % cyclic ethers together with aldehydes and olefins. The 2-methyl-5-ethyloxolane and 2,2,4,4-tetramethyloxolane were the most abundant cyclic ethers from *n*-heptane and isooctane, respectively. Experiments of Minetti et al.^{14,15} with a rapid compression machine using *n*-heptane and isooctane also indicate significant production of oxygen heterocycles ranging from oxiranes to pyrans. The latter work also revealed that oxolanes are the major heterocycles formed in cool flames, especially with isooctane fuel. It therefore appears that the reactions forming cyclic ethers are a major channel for \bullet QOOH loss, competing with the critical chain branching channel \bullet QOOH + O₂.

Although most of the recently developed kinetic models^{5,16–19} for *n*-heptane and isooctane oxidation include this reaction, more accurate rate parameters for cyclic ether formation (as well as for other \bullet QOOH elementary reactions) are needed to improve the accuracy of combustion models. Currently employed rate parameters are highly uncertain and rarely take into account the nature of the radical center or the ring size of the cyclic ethers. (Curran's mechanism,¹⁶ however, does account for the loss in entropy with increase in ring size.) Furthermore, existing models do not account for chemical activation effects, which are certainly important.²⁰

There are no direct measurements of the elementary step \bullet QOOH → cyclic ether + OH; the reported parameters in the literature for oxetane and oxirane formation rates are deduced rather indirectly. Importantly, most of the earlier works have been done before the discovery of the direct HO₂ elimination channel from RO₂.²¹ Benson estimated $A = 10^{11.5} \text{ s}^{-1}$ and $E_a \sim 14 \text{ kcal/mol}$ for oxiranes²² formation from β - \bullet QOOH based on data on the approximately thermoneutral cyclization of 3-iodopropyl radical. His²³ rate estimate for oxetanes formation from γ - \bullet QOOH is $A = 10^{11} \text{ s}^{-1}$ and $E_a = 63 \text{ kJ/mol}$ ($\sim 15 \text{ kcal/mol}$). Fish²⁴ suggested $A = 10^{11} \text{ s}^{-1}$, $E_a = 58 \text{ kJ/mol}$ ($\sim 14 \text{ kcal/mol}$) for oxiranes formation based on consideration of strain energies in cycloalkanes. Baldwin et al.²⁵ from their study of addition of HO₂ to ethylene and propene between 400 and 500 °C deduced the Arrhenius parameters $E_a = 69 \pm 5 \text{ kJ/mol}$ ($16.5 \pm 1.2 \text{ kcal/mol}$) and $\log(A/\text{s}^{-1}) = 12.0 \pm 0.5$ for oxiranes formation and determined how the A factors and activation energies change upon methyl substitution. They²⁶ also deduced the rate parameters $\log(A/\text{s}^{-1}) = 11.2 \pm 0.3$ and $E_a = 69.5 \pm 5 \text{ kJ/mol}$ ($16.6 \pm 1.2 \text{ kcal/mol}$) for cyclization of \bullet QOOH to give an oxetane and OH from studies of the addition of neopentane to slowly reacting mixtures of H₂–O₂ between 380 and 500 °C. Liquid-phase measurements were reported by Bloodworth et al.^{27,28} at 298 K for the formation of oxiranes by γ -scission from secondary β -*tert*-butylperoxyalkyl radicals and by Mill²⁹ for the decomposition of (CH₃)₂C \bullet CH₂C(CH₃)₂OOH to form 2,2,4,4-tetramethyloxetane. Bloodworth et al.^{27,28} observed a rate enhancement of approximately 20-fold with progressive introduction of each methyl group at the carbon atom bearing the peroxy groups. Recently, DeSain et al.^{30–32} made a series of measurements of HO₂ formation in reactions of ethyl, propyl, butyl, and cyclopentyl radicals with O₂. Kaiser and co-workers^{33–39} have measured alkene yields as a function of temperature and pressure for the reactions of ethyl and propyl radicals with O₂ allowing them to draw inferences about the relative importance of RO₂/ \bullet QOOH decompositions to oxiranes and to alkenes.

Besides the challenging experimental studies, several quantum chemical investigations at various levels have been done on the ethyl + O₂,^{21,40–43} propyl + O₂,^{44,45} *n*-butyl + O₂,⁴⁶ *sec*-butyl + O₂,⁴⁷ *tert*-butyl + O₂,⁴⁸ and isobutyl + O₂⁴⁸ systems. The work of Chen and Bozzelli⁴⁸ at CBS-q/MP2(fu)/6-31G* is very important for estimating the thermochemical properties of \bullet QOOH, ROOH, and RO₂ species. The important works on the rate parameters for cyclic ether formation are those of (i) Chan et al.⁴⁹ at the BH&HLYP/6-311G** level, which explores different possible oxetanes and oxiranes formation from *n*-pentyl + O₂ through isomeric pentylhydroperoxyl radicals, and (ii) DeSain et al.⁴⁶ at the QCISD(T)/6-31G(d)//B3LYP/6-31G* + Δ (MP2)(6-311++G(2df,2pd)) level on the *n*-butyl + O₂ system. The results from these two studies differ significantly, e.g. the predicted barrier heights for ring closure of a secondary radical center leading to alkyloxetane differ by $\sim 9 \text{ kcal/mol}$.^{46,49} Also, Chan et al.⁴³ treated the torsional modes as small amplitude vibrations, resulting in significant overestimation of the A factor in the rate parameters. Both studies considered only the formation of unsubstituted oxolane; very little is known about the reactions that form substituted oxolanes in large yield from primary reference fuels.

We recently obtained good results with the CBS-Q method for the thermochemical parameters of ROOH⁵⁰ and other molecular families^{51–53} including hydrocarbons with –OH, –OR, –OC(O)R, –COOH, –CHO, –COR, and –C(O)OR substituents. Our kinetic parameters for hydrogen abstraction from ROOH, computed using CBS-Q, are in reasonable agreement⁵⁴ with the sparsely available experimental data.

Herein, we investigate the formation of unsubstituted and substituted oxolanes at various levels of theory, viz., CBS-Q, CBS-QB3, QCISD/6-31G(d'), BH&HLYP/6-311G**, and B3LYP/(6-311+G(3d2f,2df,2p))/B3LYP/6-31G(d), (i) to assess the relative performance of MO- and DFT-based methods in describing the geometry as well as the barrier height of the reaction and (ii) to make an appropriate choice of the method for characterizing hydroperoxyalkyl (\bullet QOOH) radicals and their reactions. We reinvestigate the barrier heights for the formation of oxetanes and oxiranes, performing calculations at CBS-QB3 and BH&HLYP to derive a confidence level on the computationally inexpensive BH&HLYP procedure. We also study the effects of (i) ring size, (ii) variation of radical center from primary (1°) to secondary (2°) to tertiary (3°), and (iii) mono- and dialkyl substituents α to OOH group and β to the radical center.

II. Theoretical Methodology

Standard ab initio molecular orbital theory and density functional theory calculations were carried out using the GAUSSIAN 98 suite⁵⁵ of programs. Calculations on reactant radicals and open shell transition states were done within the unrestricted formalism. High-level MO calculations were done using the complete basis set methods CBS-Q and CBS-QB3 of Petersson et al.^{56,57} CBS-Q and CBS-QB3 are known for accurately predicting the thermochemistry of stable molecules. These methods aim to estimate the energy of a species at the QCISD(T) or CCSD(T) level with an infinite basis set. In this protocol, higher order correlation [MP4SDQ, QCISD(T) (or) CCSD(T)] energies are derived using a relatively small basis set, viz., CBSB4 and 6-31+G(d'), respectively, and the total energy is extrapolated to the infinite-basis-set limit using pair natural-orbital energies at the MP2 (MP2/CBSB3) correlation level and an additive correction to the QCISD(T) or CCSD(T) electron correlation level. In addition, these compound methods

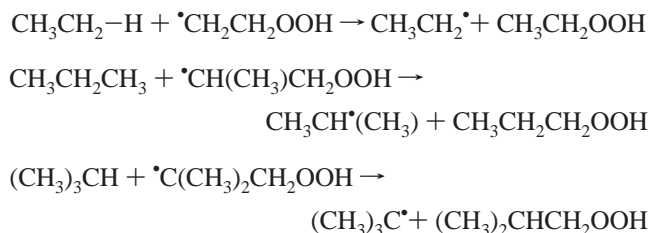
include a correction for spin contamination in open-shell species, spin-orbit corrections for atoms, and empirical bond additivity corrections to achieve improved agreement with experimental data. However, in some molecules with triple bonds the bond additivity correction is not reliable.⁵⁸ Note that unlike Pople's basis sets, the CBSB4 and CBSB3 basis sets use different polarization sets for different atoms. They can be represented in Pople's notation as 6-31+G(d(f),d,p) and 6-311+G(3d2f,-2df,2p), respectively. Basis set 6-31+G(d(f),d,p) indicates a d function on both the first and second rows, an f on selected second row atoms, and a p function on hydrogen.

In the original CBS-Q procedure, thermal corrections were derived using the HF/6-31G(d') frequencies and moments of inertia. In the present work, problems were encountered while the open-shell transition states were optimized at the HF level. Consequently, thermal corrections in our CBS-Q results were made using the scaled (0.9427) frequencies obtained at the MP2/6-31G(d') level. As recommended by Scott and Radom,⁵⁹ the frequencies obtained at B3LYP/6-31G(d) and B3LYP/CBSB7 levels are scaled by factors of 0.9613 and 0.99, respectively.

The total partition function, Q_{tot} , of all species was calculated within the framework of the rigid rotor harmonic oscillator approximation with corrections for internal rotation. The scaled harmonic vibrational frequencies and the moments of inertia were used to calculate the rotational and vibrational partition functions, entropies, and heat capacities. All torsional motions about the single bonds between polyvalent atoms were treated as hindered internal rotations. The hindrance potential for the internal rotation was obtained by optimizing the 3N-7 internal coordinates, except for the dihedral angle, which characterizes the torsional motion. The optimizations were done at the MP2/6-31G(d') level for the CBS-Q method and at the B3LYP/6-31G(d) level for the CBS-QB3 method. The dihedral angle was varied from 0° to 360° in 30° increments. The potential energy surface thus obtained was then fitted to a Fourier series $\sum_m A_m \cos(m\phi) + B_m \sin(m\phi)$ with $m \leq 8$. The procedure to obtain the hindered rotor partition function associated with this hindrance potential and its thermochemical properties is given in detail⁵¹ in our earlier publications.

The enthalpies of formation of molecules at 298.15 K were obtained from the calculated atomization energy at 0 K and experimental heats of formation of constituent atoms (ΔH^{298}) using the commonly adopted procedure⁶⁰ in the literature. The enthalpies of formation thus obtained are further improved by incorporating the spin-orbit and bond additivity corrections as recommended by Petersson et al.⁶¹

The stabilities of several β -hydroperoxyethyl radicals were determined using isodesmic reactions with the corresponding alkyl radicals:



The hydrogen-bond increment (HBI) values for the primary, secondary, and tertiary β -hydroperoxyalkyl radicals were obtained as the difference in the calculated thermochemical properties of the parent hydroperoxide and the corresponding radical.

The rate constant of the unimolecular reaction at any given temperature was calculated using the well-known transition state theory (TST) expression $k(T) = \alpha k_B T/h Q^\ddagger/Q^A \exp(-E_0/RT)$, where α is the reaction path degeneracy, Q^\ddagger 's are the total molecular partition functions, and E_0 is the zero point energy corrected barrier height. $k(T)$ was then fitted to the Arrhenius expression $k(T) = A \exp(-E_a/RT)$ to obtain the rate parameters A and E_a .

III. Results and Discussion

The reactions families considered in the present work are the formation of

- (i) five-membered cyclic ethers (oxolanes/THFs),
- (ii) four-membered cyclic ethers (oxetanes), and
- (iii) three-membered cyclic ethers (oxiranes)

from 1°, 2°, and 3° hydroperoxyalkyl radicals, $\cdot\text{CRR}'(\text{CH}_2)_n\text{-OOH}$ ($R, R' = \text{H}$ or CH_3 ; $n = 1-3$). The results of our investigation on reaction family i are given in the next section followed by families ii and iii. Besides varying the radical center from 1° to 2° to 3°, we also investigated the effect of one and two methyl substituents on the carbon containing the OOH group, namely, $\cdot\text{CH}_2(\text{CH}_2)_2\text{CRR}'\text{OOH}$ ($R, R' = \text{H}$ or Me), and on the carbon adjacent to the primary radical center, namely, $\cdot\text{CH}_2\text{CRR}'(\text{CH}_2)_2\text{OOH}$ ($R, R' = \text{H}, \text{Me}$), on the barrier height. Although such an insertion would obviously affect the reaction enthalpy, in part due to the increased strain in the resulting ring, its effect on barrier height cannot be easily guessed.

Results of earlier investigations on oxirane and oxetane formation by Pritchard and co-workers,⁴⁹ Chen and Bozzelli,⁴⁸ and DeSain et al.⁴⁶ are analyzed and combined with our results to arrive at generic rate estimation rules for these reaction families. The lack of experimental data on the kinetics of these elementary reactions prohibits a direct validation of the computed barrier heights. Consequently, indirect evidence for the accuracy of the chosen levels of treatment is presented through thermochemistry comparison. For the effective use of this investigation by the modeling community, we compiled the rate parameters (A and E_a), new hydrogen-bond increment (HBI) values for β -hydroperoxyalkyl radicals, and ring strain corrections (RSC) for the cyclic ethers.

Formation of Oxolanes from δ -Hydroperoxybutyl Radical.

Tables 1 and 2 give the barrier heights at 0 K (E_0), reaction coordinate geometry, and magnitude of the imaginary frequency at the transition state together with other characteristics for the reactant radicals and transition structures involved in 5-membered ring formation. The most surprising observation is the consistent 5–6 kcal/mol difference between barrier height predictions at the CBS-Q (MO) and B3LYP/CBSB3//B3LYP/6-31G(d) (DFT) levels. Although it is known in the literature that B3LYP underestimates the barrier heights in reactions involving H migration, the underestimation is not usually so large. Earlier we reported⁵⁰ a difference of ~ 2 kcal/mol in the computed barrier height at these two levels for hydrogen abstraction by HO_2 from alkanes.

The magnitude of the imaginary frequency at the MP2 level is consistently around 1550 cm^{-1} , while at the B3LYP level it is $\sim 660 \text{ cm}^{-1}$. Moreover, the MP2 frequency increases when the radical is varied from 1° to 2° to 3°, while the B3LYP frequency decreases by about the same amount along the series, suggesting a significantly different contribution of the internal coordinates to the reaction coordinate.

A closer examination revealed that the observed discrepancies could be due to the differences in the computed TS geometries & reaction coordinates. The reaction here is exothermic and

TABLE 1: Oxolane (THF) Formation Barrier Height E_0 (in kcal/mol), Reaction Enthalpy ΔH_R at 0 K (in kcal/mol), Reactive Moiety Geometry (bond length in Å), Imaginary Frequency (ν_i in cm^{-1}) at the Transition State, and the Low-Frequency (ν_{HIR} in cm^{-1}) Torsional Vibrations Treated as Hindered Rotations in the Reactant and the Transition State^a

method	E_0	ΔH_R	transition state					reactant	
			O—O	C—O	ν_i	OO ν_{HIR}	$\langle S^2 \rangle$	ν_{HIR}	$\langle S^2 \rangle$
*CH ₂ CH ₂ CH ₂ CH ₂ OOH → Oxolane + OH									
B3LYP ^c	11.1	−34.1	1.664	2.137	678	92	0.790	78, 95, 124, 147, 199	0.754
CBS-Q ^b	17.0 [16.1]		1.564	1.931	1541	125	1.035	82, 104, 150, 58, 173	0.763
HL ^d	14.0								
CBS-QB3	14.6	−35.6	1.666	2.166	667	62	0.791	77, 91, 116, 145, 173	0.754
QCISD ^e	15.6		1.690	2.111			1.261		0.763
BH&HLYP ^f	16.3	−40.5	1.670	2.160	834	117	0.916		
B3LYP/CBSB3//MP2/6-31G(d')	16.2								

^a The number in square brackets corresponds to CBS-Q barrier height with B3LYP/CBSB7 ZPE correction. $\langle S^2 \rangle$ refers to spin contamination at the level of geometry optimization. ^b CBS-Q//MP2/6-31G(d'). ^c B3LYP/CBSB3//B3LYP/6-31G(d). ^d QCISD(T)/6-31G**//B3LYP/6-31G*+ΔMP2(6-311++G(2df,2pd)), DeSain et al.⁴⁶ ^e QCISD/6-31G(d')//QCISD/6-31G(d'). ^f BH&HLYP/6-311G**, Chan et al.⁴⁹

TABLE 2: 2-Methyl- and 2,2-Dimethyloxolane Formation Barrier Heights E_0 and Reaction Enthalpies ΔH_R at 0 K (both in kcal/mol), Reactive Moiety Geometries (bond length in Å), Imaginary Frequencies (ν_i in cm^{-1}) at Transition States, and the Low-Frequency (ν_{HIR} in cm^{-1}) Torsional Vibrations Treated as Hindered Rotations in the Reactants and Transition States^a

method	E_0	ΔH_R	transition states					reactants		
			O—O	C—O	ν_i	ν_{HIR}		$\langle S^2 \rangle$	ν_{HIR}	$\langle S^2 \rangle$
CH ₃ *CHCH ₂ CH ₂ CH ₂ OOH → 2-Methyloxolane + OH										
B3LYP ^c	9.8	−34.4	1.664	2.173	637	110	145	0.786	46, 71, 99, 110, 125, 196	0.754
CBS-Q ^b	15.5 [14.7]		1.558	1.938	1565	130	180	1.026	52, 74, 118, 139, 162, 173	0.763
CBS-QB3	10.3 ^e {12.8}	−37.4	1.663	2.208	624	82	110	0.786	44, 69, 98, 105, 119, 177	0.754
BH&HLYP ^d	15.5	−41.7	1.660	2.179	850	96	140	0.899	44, 71, 114, 120, 149, 190	0.756
(CH ₃) ₂ C*CH ₂ CH ₂ CH ₂ OOH → 2,2-Dimethyloxolane + OH										
B3LYP ^c	8.2	−34.0	1.665	2.202	615	89	147, 150	0.784	43, 58, 84, 119, 127, 140, 202	0.754
CBS-Q ^b	13.1 [12.4]		1.555	1.946	1581	127	192, 193	1.021	51, 63, 118, 143, 156, 159, 172	0.763
CBS-QB3	8.4 ^e {10.9}	−38.5	1.664	2.238	596	45	143, 147	0.782	37, 55, 98, 121, 123, 136, 183	0.754
BH&HLYP ^d	14.0	−42.0	1.654	2.191	859	99	142, 149	0.887	44, 60, 108, 129, 134, 146, 192	0.756

^a The CBS-Q numbers in square brackets correspond to CBS-Q barrier heights with B3LYP/CBSB7 ZPE corrections. The CBS-QB3 numbers in braces come from correcting the erroneously computed $\Delta\Delta E(\text{Emp})$ by +2.5 kcal/mol (see the text). $\langle S^2 \rangle$ refers to spin contamination at the level of geometry optimization. ^b CBS-Q//MP2/6-31G(d'). ^c B3LYP/CBSB3//B3LYP/6-31G(d). ^d BH&HLYP/6-311G**. ^e CBS-QB3 extrapolation term is unreliable for these cases (see the text).

the exothermicity increases from 1° to 2° to 3°; in accordance with Hammond's postulate, the transition state geometry is close to that of the reactant, though in a cyclic geometry, and with the radical bearing C approximately collinear with the O—O bond. However, at the DFT level, the O—O bond dissociation is more advanced [$\delta(\text{O—O})$ from reactant to TS is 0.212 Å], while at the MP2 level the C—O bond formation is more advanced (the C—O bond lengths in the B3LYP and MP2 transition states differ by 0.236 Å). The eigenvectors corresponding to the negative eigenvalue of the force constant matrix show the reaction coordinate to be primarily the asymmetric C•••O•••O stretch in both cases, as expected. However, the contribution of the forming C—O and breaking O—O bonds differs between the two levels of theory.

Earlier investigations on formation of oxolanes and oxetanes from *QOOH have employed B3LYP⁴⁶- or BH&HLYP⁴⁹-optimized geometries and no comparison exists with MP2 geometries. As known in the literature, increasing the size of the basis set at the B3LYP level does not have any significant effect on the optimized geometry. The common consensus is that the geometries, though not the magnitude of the barrier heights, obtained at the B3LYP level are often more reliable than at MP2. To resolve the differences in geometry, we reoptimized the transition state leading to oxolane at the QCISD/6-31G(d') level. We assume here that the geometry obtained at this level could be taken as a standard. Such an assumption is justifiable, due to the fact that the G2-RAD⁶² method with QCISD/6-31G(d) optimization is known to perform better than

G2 (MP2(fu) optimization) for radicals. The geometry obtained at this higher level MO theory is close to that obtained using B3LYP. Consequently, we conclude that the B3LYP geometry is more reliable than the MP2. However, the computed barrier height (15.59 kcal/mol) at QCISD/6-31G(d') is energetically close to that of the CBS-Q predictions, suggesting a probable underestimation of the barrier height at the B3LYP level.

Brinck et al.⁶³ found that the well-established O—H bond dissociation energy (BDE) in H₂O₂ is underestimated by 7.5 and 5.5 kcal/mol, respectively, at the B3LYP/6-31+G(d,p) and B3LYP/6-311+(2df,2p) levels. One of us⁶⁴ has earlier demonstrated similar underestimation of hydroperoxide O—H BDEs using other DFT functionals. Here we computed the O—O BDEs in various ROOH using B3LYP/CBSB3//B3LYP/6-31G(d), BH&HLYP/6-31G**, CBS-Q, and CBS-QB3 (Table 3). Although the experimental heats of formation of ROOH are not precisely established, the accepted literature values⁴⁵ based on G2 calculations for $\Delta_f H^{298}$ are as follows: CH₃OOH, −31.8 kcal/mol; (CH₃)₂CHOOH, −49.0 kcal/mol; and (CH₃)₃COOH, −58.4 kcal/mol. Combination of these values together with the experimental $\Delta_f H^{298}$ values⁶⁵ for methoxy, isopropoxy, and *tert*-butoxy radicals yields O—O BDEs in close agreement with the CBS-Q and CBS-QB3 methods. However, attention must be paid to the orientation of the odd electron in the unsymmetrical alkoxy radicals such as ethoxy and isopropoxy. Different levels of treatment (CBS-Q, B3LYP) results in different most favored conformations. It must be noted that optimizations at single

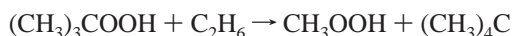
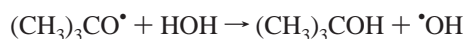
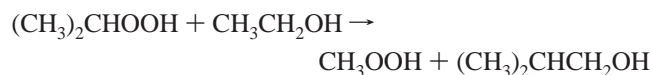
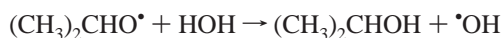
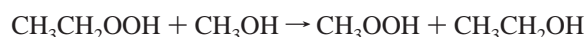
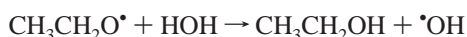
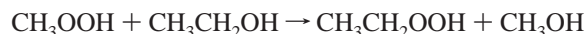
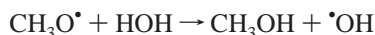
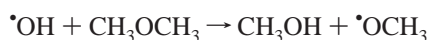
TABLE 3: Calculated Peroxy O–O Bond Dissociation Enthalpies (BDE 298 K in kcal/mol) in Hydroperoxides at B3LYP/CBSB3//B3LYP/6-31G(d), BH&HLYP/6-311G, CBS-Q, and CBS-QB3 Levels Compared with Literature Derived Values (see text)**

species	B3LYP	BH&HLYP ^a	BH&HLYP ^b	CBS-Q	CBS-QB3	lit. value
CH ₃ OOH	37.6	27.4	47.6	45.5	45.6	45.2
EtOOH ^c	38.3	28.5	48.4	46.1	46.3	45.1
<i>i</i> -PrOOH ^d	38.1	28.2	49.1	46.5	46.6	45.8
<i>t</i> -BuOOH	38.0	28.3	50.7	46.4	46.8	46.1

^a Calculated directly using BH&HLYP/6-311G** energies. ^b Calculated using ROOH, RO•, and •OH heats of formation derived by means of isodesmic reactions (see the text). ^c The lowest energy conformer of ethoxy at the BH&HLYP and CBS-Q levels is the one where the odd electron is trans to the β C–C bond and there is a local C2 axis of rotation. At the B3LYP level it is the one where the odd electron is gauche to the β C–C bond. ^d The lowest energy conformer of isopropoxy at the BH&HLYP and CBS-Q levels is the one where the odd electron is trans to the β C–H bond and there is a local C2 axis of rotation. At the B3LYP level it is the one where the odd electron is gauche to the β C–H bond.

configuration levels do not account for the “nondynamic correlation” inherent in these radicals.

B3LYP and BH&HLYP O–O BDEs are underestimated by 8 and 18 kcal/mol, respectively (Table 3), when calculated directly using the B3LYP/CBSB3//B3LYP/6-31G(d) and BH&HLYP/6-311G** energies. These large errors in the BDEs indicate the poor description of bonds at the B3LYP and BH&HLYP levels, which need to be improved by using isodesmic reactions. Calculating heats of formation of ROOH, RO•, and •OH using the following isodesmic reactions,



gives values that are in good agreement with experimental heats of formation (Supporting Information, Table A). The resulting BH&HLYP BDEs now are in better agreement with the literature derived results (Table 3).

It is clear that in the absence of isodesmic corrections, direct DFT BDEs can be seriously inaccurate. Presumably this error also affects TS calculations that involve bond breaking, such as the title reaction. However, as discussed above, DFT geometries appear to be accurate. Therefore, a meaningful and consistent method for describing chemical reactions from hydroperoxyalkyl radicals should involve a geometry optimiza-

tion at the DFT level coupled with an energy calculation using one of the compound methods such as CBS-QB3 or G3X.⁶⁶ In the present work we restrict ourselves to the CBS-QB3 method.

However, CBS-QB3 is a computationally expensive method, feasible only for systems consisting of hardly 10 or fewer heavy atoms. It is therefore worthwhile to identify an alternative and relatively inexpensive method for systematic characterization of reactions important in low-temperature oxidation. The literature shows^{67,68} that the BH&HLYP functional often performs better than B3LYP in predicting transition state properties, and BH&HLYP often gives more accurate barrier heights than B3LYP, though less accurate bond energies and energies of reaction.⁶⁹ BH&HLYP was used extensively in previous work on this system.⁴⁹ In the present work, we reexamine its predictive ability in describing the thermodynamic and kinetic parameters of the title reaction.

As can be seen from Table 1, the BH&HLYP barrier height is in good agreement with those of QCISD/6-31G(d') and CBS-QB3, despite the fact that it does not give accurate thermochemistry. In estimating the heats of reaction for cyclization to form oxolane, CBS-QB3 gives values that are in good agreement with empirical estimates, while BH&HLYP results are overestimated by about 5 kcal/mol. Consequently, although BH&HLYP gives a good estimate for the barrier to the forward direction, the reverse reaction barrier is overestimated by ~5 kcal/mol. B3LYP, however, happens to predict the heats of cyclization reaction quite well (Tables 1 and 2). The consequence of this is that both forward and reverse barrier heights for B3LYP are too low.

A part of the 2.5 kcal/mol difference in CBS-Q and CBS-QB3 barrier heights (Table 1) for oxolane formation stems from the zero point energy corrections. Use of MP2/6-31G(d')-scaled frequencies results in positive (viz., 0.85, 0.5 kcal/mol) ZPE corrections, in contrast to the general understanding that ZPE drops in a dissociative transition state. The CBS-Q barrier height with scaled (0.99) B3LYP/CBSB7 ZPE corrections is in better agreement with CBS-QB3 predictions (Table 1). The surprisingly close agreement between the CBS-Q and B3LYP/CBSB3//MP2/6-31G(d') barriers is probably just fortuitous.

The salient observations from the above comparison of MO- and DFT-based methods for oxolanes formation are as follows:

(1) B3LYP/6-31G(d) describes the TS geometry better than MP2, if one assumes the geometry obtained at the QCISD/6-31G(d') level as the standard.

(2) The barrier height obtained from all of the methods except B3LYP//B3LYP is in agreement that $14 < E_0 < 16.5$ kcal/mol.

(3) B3LYP not only underestimates the barrier height but also the experimentally known BDEs in alkylhydroperoxides.

(4) On the basis of the performance for oxolanes formation, BH&HLYP could be a method of choice in regard to the computational cost, particularly for geometry optimizations and frequency calculations. However, caution must be exercised while using BH&HLYP, since it does not accurately compute the heats of reaction.

Formation of Oxolanes from Secondary and Tertiary Radicals: Barrier Height Trends. The formation of substituted oxolanes from secondary and tertiary radicals has not been investigated previously at high levels of MO theory. Our calculations showed the following:

(1) Using the CBS-Q and B3LYP methods (Table 2), we found the barrier height consistently decreases by ~1.5 kcal/mol from 1° to 2° and from 2° to 3°. This decrease is consistent with the change in the heat of reactions.

TABLE 4: Oxetane and Oxirane Formation Reaction Enthalpies ΔH_R at 0 K (in kcal/mol), Reactive Moiety Geometry (bond length in Å), the Imaginary Frequencies (ν_i in cm^{-1}) at Transition States, and the Magnitude of Low-Frequency (ν_{HIR} in cm^{-1}) Torsional Vibrations Treated as Hindered Rotations in the Reactants and Transition States^a

reactants	method	ΔH_R	transition states						reactants	
			O–O	C–O	ν_i	ν_{HIR}		$\langle S^2 \rangle$	ν_{HIR}	$\langle S^2 \rangle$
Oxetane Formation										
$\cdot\text{CH}_2\text{CH}_2\text{CH}_2\text{OOH}$	CBS-QB3	−16.4	1.692	2.004	784	140	N/A	0.794	47, 111, 125, 195	0.754
	BH&HLYP ^b	−20.8	1.703	2.024	874	98	N/A	0.935	110, 113, 147, 202	0.755
$\text{CH}_3\cdot\text{CHCH}_2\text{CH}_2\text{OOH}$	CBS-QB3	−19.3	1.694	2.046	723	96	136	0.790	41, 83, 99, 117, 190	0.754
	BH&HLYP ^b	−23.7	1.692	2.052	875	104	137	0.916	36, 97, 106, 126, 199	0.756
$(\text{CH}_3)_2\cdot\text{CCH}_2\text{CH}_2\text{OOH}$	CBS-QB3	−21.2	1.690	2.076	680	104	138, 148	0.785	40, 86, 94, 112, 119, 179	0.754
	BH&HLYP ^b	−25.0	1.679	2.064	889	104	142, 155	0.897	41, 91, 103, 117, 130, 191	0.756
Oxirane Formation										
$\cdot\text{CH}_2\text{CH}_2\text{OOH}$	CBS-QB3	−16.0	1.756	1.921	738	125	N/A	0.816	118, 163, 221	0.754
	BH&HLYP ^b	−18.7	1.772	1.983	655	14	N/A	1.011	136, 171, 222	0.755
$\text{CH}_3\cdot\text{CHCH}_2\text{OOH}$	CBS-QB3	−17.5	1.759	1.947	688	133	108	0.810	62, 89, 164, 201	0.754
	BH&HLYP ^b	−20.3	1.752	1.997	682	86	93	0.980	67, 87, 168, 220	0.756
$(\text{CH}_3)_2\cdot\text{CCH}_2\text{OOH}$	CBS-QB3	−18.7	1.759	1.972	641	118	82, 88	0.803	38, 82, 105, 139, 205	0.754
	BH&HLYP ^b	−21.2	1.739	2.010	702	42	86, 105	0.954	47, 99, 118, 151, 222	0.756

^a $\langle S^2 \rangle$ refers to spin contamination at the level of geometry optimization. ^b BH&HLYP/6-311G**.

(2) Our BH&HLYP barrier heights for oxolane and 2-methyloxolane formation are slightly different (within 0.5 kcal/mol) than those of Chan et al.⁴⁹ In contrast to their calculations, which yielded approximately the same barrier (16 kcal/mol) for both the unsubstituted and substituted case, our barrier heights showed a 1.2 kcal/mol decrease from oxolane to 2-methyloxolane formation. We did calculations on several additional systems and found the same trend in going from 1° to 2° to 3° in BH&HLYP as in CBS-Q and B3LYP (Tables 1 and 2). In all cases, the BH&HLYP barrier is consistently close to that from CBS-Q.

(3) At the CBS-QB3 level, however, the decrease in barrier height on going from 1° to 2° is much larger than with the other methods: ~ 4.4 kcal/mol. Analysis of the relative barrier height at each component level of the CBS-QB3 method, (viz., CCSD-(T)/6-31+G(d'), MP4SDQ/CBSB4, and MP2/CBSB3) yielded a consistent difference of only ~ 1.6 kcal/mol, suggesting problems with the CBS extrapolation procedure (see the section on the source of the problem in some CBS-QB3 calculations below).

Formation of Oxetanes and Oxiranes. The optimized geometrical parameters of the TS's for formation of oxiranes and oxetanes and the magnitude of the low-frequency vibrations in the reactants are tabulated in Table 4 together with heats of reaction. Comparisons of barrier heights with literature values are presented in Table 5. The following observations can be made from Tables 4 and 5:

(1) Formation of oxetanes and oxiranes is consistently more exothermic by, respectively, ~ 4.5 and ~ 2.5 kcal/mol for BH&HLYP compared to CBS-QB3. Again, CBS-QB3 heats of reaction are in good agreement with empirical estimates.

(2) At the CBS-QB3 level, the reactions forming oxetanes have the highest activation barrier and the reactions forming oxolanes have the lowest activation barriers, for a given nature of the radical center. The reactions forming oxiranes have intermediate barriers: oxetanes > oxiranes > oxolanes. This behavior does not parallel the increasing strain at the transition state with decreasing ring size.

(3) At the BH&HLYP/6-311G** level, the barrier heights for oxiranes and oxolanes exhibit a different trend: oxetanes > oxolanes > oxiranes. However, the magnitude of the calculated barrier height is in good agreement (within ± 0.5 kcal/mol) with CBS-QB3 estimates for oxirane formation and differs systematically by about 2 kcal/mol for oxetane formation.

(4) Baldwin et al.²⁵ and Benson²² estimated nearly the same activation energy for both oxetane and oxirane formation. In contrast to their estimates, at both CBS-QB3 and BH&HLYP levels, the E_0 for oxetane formation is significantly higher than that for oxirane.

(5) At both these levels, for a given particular ring size, the barrier height for ring closure decreases from primary to secondary to tertiary radical and the decrease is by about the same magnitude. In this regard, the barrier heights calculated by DeSain et al. for $\text{CH}_3\text{CH}\cdot\text{CH}_2\text{CH}_2\text{OOH} \rightarrow$ 2-methyloxetane (30.3 kcal/mol) and by Chen and Bozzelli⁴⁸ for $(\text{CH}_3)_2\text{C}\cdot\text{CH}_2\text{OOH} \rightarrow$ 2,2-dimethyloxirane (19.3 kcal/mol) seem doubtful.

(6) In accordance with the liquid-phase experimental results of Bloodworth et al.,²⁸ progressive substitution of methyl groups on the carbon bonded to the peroxy oxygen results in a systematic decrease in the barrier height (15.5 \rightarrow 13.7 \rightarrow 11.4 kcal/mol) for oxirane formation.

(7) Optimized geometries at both the B3LYP/CBSB7 and BH&HLYP/6-311G** levels exhibit the same trend:

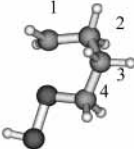
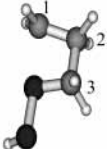
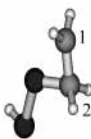
cleaving O–O bond length decreases and the forming C–O bond length increases from 3- to 4- to 5-membered TS, and in every case, the length of the forming C–O bond increases from 1° to 2° to 3°.

(8) The reactions leading to oxolanes (5-membered rings) are more exothermic compared to oxetanes (4-membered rings), which in turn are slightly more exothermic compared to oxiranes (3-membered rings).

Source of the Problem in Some CBS-QB3 Calculations.

Having seen a relatively good agreement between CBS-QB3 and BH&HLYP for the barrier heights of the reactions forming oxetanes and oxiranes, which contrasts sharply with our results on reactions that form substituted oxolanes (Table 2), we reanalyzed the various quantities that contribute to the CBS-QB3 barrier height: $\Delta\Delta E(\text{MP2})$, $\Delta\Delta E(\text{MP34})$, $\Delta\Delta E(\text{CCSD(T)})$, $\Delta\Delta E(\text{CBS})$, $\Delta\Delta E(\text{Int})$, and $\Delta\Delta E(\text{Emp})$ (Supporting Information, Table B) for all the reactions. $\Delta\Delta$ stands for the difference between the reactant and the corresponding transition state and is therefore its contribution to the barrier height. We observed an overstabilization of $\Delta\Delta E(\text{Emp})$, viz., extrapolation of infinite order pair energies, by 2.29 kcal/mol for formation of substituted oxolanes from $\text{CH}_3\text{CH}\cdot(\text{CH}_2)_3\text{OOH}$, $(\text{CH}_3)_2\text{C}\cdot(\text{CH}_2)_3\text{OOH}$, and $\cdot\text{CH}_2\text{C}(\text{CH}_3)_2(\text{CH}_2)_2\text{OOH}$ radicals (Supporting Information, Table B). In all other systems, the contribution of

TABLE 5: Barrier Heights (in kcal/mol) for Oxolane, Oxetane, and Oxirane Formation from the Corresponding Hydroperoxyalkyl Radicals Together with Literature Data^h

Oxolane (THF) Formation (Present work)							
	Sub 1	Sub 2	Sub 4	CBS-QB3	BH&HLYP ^b	B3LYP ^a	CBS-Q
	--	--	--	14.6 (14.0 ^c)	16.7	10.3	17.0
	methyl	--	--	12.8 ^c	15.5	8.7	15.5
	dimethyl	--	--	10.9 ^c	14.0	7.5	13.1
	--	methyl	--	14.2	16.5	10.2	
	--	dimethyl	--	13.6 ^c	15.4	9.0	
	--	--	methyl	15.0	17.4	11.0	16.6
--	--	dimethyl	14.7	16.7	10.2		
Oxetane Formation (Present Work together with Literature Data)							
	Sub 1	Sub 2	Sub 3	CBS-QB3	BH&HLYP ^b	Chan ^d	DeSain ^e
	--	--	--	21.5	23.6	23.8	23.4 ^f
	methyl	--	--	19.0	21.3		30.3
	ethyl	--	--			21.5	
	dimethyl	--	--		16.5	19.6	19.6
	--	methyl	--			22.5	20.7
	--	dimethyl	--		19.5	21.0	20.1
--	--	methyl			22.5	22.2	
--	--	dimethyl			21.3		
Oxirane Formation (Present Work together with Literature Data)							
	Sub 1	Sub 2	Chen ^g	CBS-QB3	BH&HLYP ^b	Chan ^d	DeSain ^e
	--	--		16.1	15.6	15.5	
	methyl	--		15.3	14.3		15.1 ^f
	ethyl	--					14.3
	propyl	--				13.8	
	dimethyl	--	19.3	12.3	12.9		12.3
	ethyl	--				13.2	
	methyl	--					
	--	methyl		14.5	13.7		15.3 ^f
	--	ethyl					14.4
	methyl		methyl				12.7
--	dimethyl	15.58	12.8	11.4		11.8	

^a B3LYP/CBSB7. ^b BH&HLYP/6-311G**. ^c Corrected by 2.5 kcal/mol; see the text. ^d BH&HLYP, Chan et al.⁴⁹ ^e QCISD(T)/6-31G**//B3LYP/6-31G* + ΔMP2(6-311++G(2df,2pd), De Sain et al.⁴⁶ ^f QCISD(T)/6-311G**//B3LYP/6-31G* + ΔMP2(6-311++G(2df,2pd), DeSain et al.⁴⁶ ^g CBS-Q/MP2(full)/6-31G*, Chen and Bozzelli.⁴⁸ ^h "Sub 1" indicates substitution at carbon 1, "Sub 2" indicates substitution at carbon 2, and "Sub 3" indicates substitution at carbon 3.

the $\Delta\Delta E(\text{Emp})$ to the barrier height is close to zero. The extrapolation procedure seems to have run into problems, and $\Delta\Delta E(\text{Emp})$ is not reliable in the cases cited.

It has previously been noted⁵⁸ that $\Delta E(\text{Emp})$ is quite sensitive to errors in the population localization method employed. Presumably, this motivated the switch from the method of Pipek and Mezey⁷⁰ (CBSExtrap=POP) used by default for CBS-Q to the minimum population localization method of Montgomery et al.⁷¹ (Gaussian keyword MINPOP) as the default in the newer CBS-QB3. In the cited cases, we suspect that the CBS-QB3 $\Delta E(\text{Emp})$ is computed erroneously, despite using the MINPOP algorithm. It appears that the empirical correction in the CBS methods needs reexamination. Correcting the $\Delta\Delta E(\text{Emp})$ in the cited cases by +2.5 kcal/mol results in better agreement between CBS-QB3 and BH&HLYP (and CBS-Q) levels. However, a consistent difference of ~ 2 kcal/mol still prevails in the magnitude of the barrier heights computed at the CBS-QB3 and BH&HLYP levels (Table 5), and we believe this gives a fair indication of the uncertainty in the theoretical barrier heights.

Effect of Mono- and Dialkyl Substitution away from the Radical Center on Cyclic Ether Formation Barrier Heights. Figure 2 shows the variation of barrier heights with heats of reaction for substituted oxetanes and oxiranes formation. In the

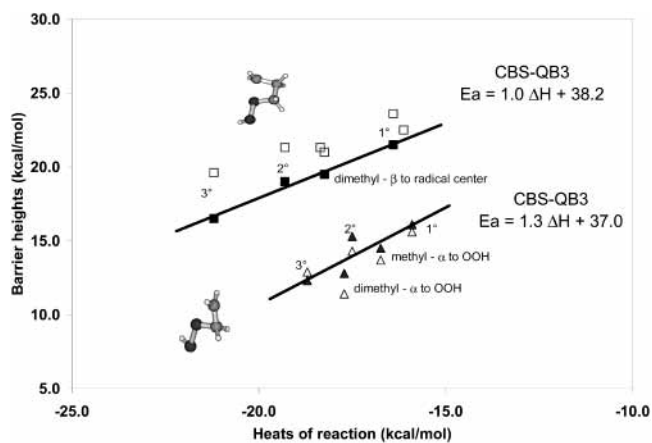


Figure 2. Evans–Polanyi plot of CBS-QB3 (▲, ■) and BH&HLYP/6-311G** (△, □) barrier heights (in kcal/mol) vs CBS-QB3 heats of reactions (in kcal/mol) leading to oxirane (▲, △) and oxetane (■, □) rings. BH&HLYP heats of reactions are not used because of their 5 kcal/mol overestimation. For those BH&HLYP data points where CBS-QB3 heats of reactions are not available, the X-axis values are estimated using group additivity.

case of oxiranes, increased alkyl substitution α to OOH (or equivalently β to the radical center) lowers the barrier height

TABLE 6: Effect of Alkyl Substitution on 5-Membered Cyclic Ether Formation Barrier Heights E_0 (in kcal/mol), Reaction Enthalpies ΔH_R at 0 K (in kcal/mol), Reactive Moiety Geometries (bond length in Å), Imaginary Frequencies (ν_i in cm^{-1}) at Transition States, and the Low-Frequency (ν_{HIR} in cm^{-1}) Torsional Vibrations Treated as Hindered Rotations in the Reactant and Transition Structures^a

method	E_0	ΔH_R	transition state parameters						reactant parameters	
			OO	CO	ν_i	ν_{HIR}		$\langle S^2 \rangle$	ν_{HIR}	$\langle S^2 \rangle$
*CH ₂ CH ₂ CH ₂ CH(CH ₃)OOH → 2-Methyloxolane										
CBS-Q	16.6		1.562	1.930	1547	172	235	1.032	75, 89, 141, 149, 213, 261	0.763
CBS-QB3	15.0	35.8	1.665	2.170	653	117	237	0.789	72, 104, 109, 117, 211, 256	0.754
BH&HLYP	17.4	41.1	1.668	2.164	832	141	234	0.914	77, 109, 113, 128, 216, 261	0.755
*CH ₂ CH ₂ CH ₂ C(CH ₃) ₂ OOH → 2,2-Dimethyloxolane										
CBS-QB3	14.7	36.9	1.667	2.169	650	164	220, 226	0.789	65, 92, 106, 126, 209, 239, 254	0.754
BH&HLYP	16.7	43.1	1.675	2.164	818	153	233, 262	0.923	63, 95, 116, 147, 233, 252, 275	0.755
*CH ₂ CH(CH ₃)CH ₂ CH ₂ OOH → 3-Methyloxolane										
CBS-QB3	14.2	36.3	1.663	2.166	662	87	214	0.789	74, 78, 125, 154, 183, 242	0.754
BH&HLYP	16.5	42.0	1.667	2.157	839	116	245	0.912	78, 83, 145, 159, 194, 252	0.755
*CH ₂ C(CH ₃) ₂ CH ₂ CH ₂ OOH → 3,3-Dimethyloxolane										
CBS-QB3	11.1 ^b {13.6}	37.4	1.658	2.157	661	90	246, 263	0.788	69, 71, 130, 151, 182, 243, 273	0.754
BH&HLYP	15.4	43.1	1.661	2.144	851	117	259, 274	0.905	74, 76, 151, 157, 196, 253, 285	0.755

^a The CBS-QB3 number in braces comes from correcting the erroneously computed $\Delta\Delta E(\text{Emp})$ by +2.5 kcal/mol (see the text). $\langle S^2 \rangle$ refers to spin contamination at the level of geometry optimization. ^b CBS-QB3 extrapolation term unreliable for this case, see text.

consistently by 2 kcal/mol. In the oxetane case, mono- and dimethyl substitutions α to OOH and β to the radical center lower the barrier heights consistently by 1 kcal/mol (see also Table 5).

On the other hand, in oxolane case, substitution of one or two methyl groups α to the OOH group and β to the primary radical center does not have much influence on the barrier height (Table 6).

We can see that, for both oxirane and oxetane, $\delta E_a/\delta\Delta H_R \approx 1$. Such a high slope is unexpected, since usually exothermic reactions have Evans–Polanyi slopes ≤ 0.5 . It is possible that this correlation reflects some other physical phenomena. The implication of this Evans–Polanyi slope of nearly 1 is that the barrier for the reverse reaction $\text{OH} + \text{cyclic ether} \rightarrow \text{*QOOH}$ is insensitive to alkyl substitutions, even if they change the thermochemistry. Unfortunately, there is no known experimental result that could confirm this prediction.

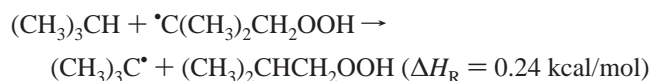
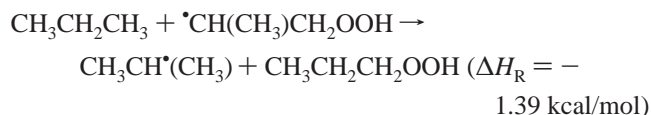
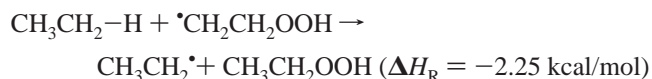
Thermochemical Values for Hydroperoxyalkyl Radicals (*QOOH) and Cyclic Ethers. Thermochemical parameters for alkylhydroperoxy radicals calculated with CBS-QB3 and CBS-Q are given in Tables 7 and 8 together with THERM predictions using group additivity (GA) and hydrogen-bond increment (HBI).⁷² It should be stated that the available HBI values are probably no more accurate than the present calculations, as they come either from very rough estimates or nearly the same level of theory as employed in this work. Often they are derived from a very narrow test set or even from calculations on a single species. Thermodynamic parameters of the parent hydroperoxides ROOH also are not well defined experimentally, adding uncertainty in the GA predictions. Consequently, the present comparison could only help us to evaluate them.

The radical center in *CRR'(CH₂)_nOOH ($n = 2, 3$) species is far away from the OOH group and so it is acceptable to use the HBIs for alkyl radicals (we used Bozzelli's HBI value for 3° bonds, though the correct value for this group is the subject of long-standing debate⁷³). For these cases, we also did estimations using Benson's GA values for free radicals.

The GA predictions are generally in good agreement with our calculated results for the unsubstituted and monomethyl substituted radicals. The observed discrepancies in entropy (up to ~ 2 cal/mol K) and low temperature heat capacities arise from

their strong dependence on the magnitude of the low-frequency vibrations and hindrance potentials.

For *CRR'CH₂OOH radicals, Benson has not reported a value for the {C/H₂/O/C*} group. The alkyl radical HBI values are not appropriate for estimation of this β -hydroperoxyalkyl radical thermochemistry, since we calculate that a β -OOH group increases the bond strength of primary and secondary C–H bonds:



We therefore arrived at new CJCOOH, CCJCOOH, and C2CJCOOH HBIs using our CBS-QB3 thermochemical properties of CH₃CH₂OOH, CH₃CH₂CH₂OOH, and (CH₃)₂CHCH₂OOH, respectively (Table 8).

For a few of the cyclic ethers, experimental thermochemical data are available and they are in excellent agreement with our calculated values (Tables 9 and 10). Group additivity predictions, however, show considerable deviations, especially in the case of oxolane and oxetane. This immediately makes one suspect the ring strain correction (RSC) values used in the GA estimate. The ring corrections used in the S&P program⁷⁴ are the ones reported recently by Cohen⁷⁵ and are often taken as equal to those of the corresponding cycloalkanes.

We improved the ring strain correction values based on thermochemical properties obtained from CBS-QB3 calculations. While the S and $C_p(T)$ correction factors for the unknown groups were taken as the averages of the differences between the ab initio calculations and the known constituent group values, additional non-next neighbor corrections were incorporated for the enthalpy term. The unsubstituted oxolane, oxetane,

TABLE 7: Thermochemical Properties of δ -Hydroperoxyalkyl Radicals (*QOOH) That Form 5-Membered Ring Cyclic Ethers^a

method	ΔH^{298}	S^{298}	$C_p(T)$						
			300	400	500	600	800	1000	1500
*CH ₂ CH ₂ CH ₂ CH ₂ OOH									
CBS-QB3	-0.10	97.16	29.98	36.64	42.48	47.33	54.77	60.21	68.64
CBS-Q	-0.38	96.94	30.79	37.68	43.60	48.46	55.83	61.17	69.35
THERM ^b	-0.86	96.65	30.52	37.26	43.06	48.02	55.58	61.45	
S&P ^c	-0.40	97.00	30.50	36.80	42.80	47.40	54.90	59.80	
CH ₃ *CHCH ₂ CH ₂ OOH									
CBS-QB3	-8.20	106.73	34.66	42.52	49.65	55.71	65.12	72.02	82.66
CBS-Q	-9.18	106.95	35.81	43.80	50.97	57.00	66.30	73.08	83.44
THERM;S ^b	-8.44	107.10	35.29	43.24	50.12	56.38	66.06	73.08	
THERM;RCCJC ^b	-8.44	107.79	35.25	42.80	49.73	55.87	65.46	72.89	
S&P ^c	-8.00	107.30	35.70	43.30	50.50	56.10	65.40	71.80	
(CH ₃) ₂ *CCH ₂ CH ₂ OOH									
CBS-QB3	-17.00	115.54	38.54	47.90	56.49	63.82	75.26	83.66	96.55
CBS-Q	-18.16	114.68	40.64	49.76	58.21	65.41	76.65	84.88	97.43
THERM ^b	-17.56	113.26	41.24	49.98	57.99	65.11	76.32	84.99	
S&P ^c	-16.50	114.60	41.50	50.80	59.00	65.90	77.00	84.60	
*CH ₂ CH ₂ CH ₂ CH(CH ₃)OOH									
CBS-QB3	-9.57	103.84	37.54	45.28	52.10	57.80	66.60	73.05	83.13
CBS-Q	-9.03	104.82	38.31	46.14	52.97	58.65	67.40	73.80	83.71
THERM ^b	-10.16	105.46	36.52	44.89	52.26	58.11	67.30	74.29	
*CH ₂ CH ₂ CH ₂ C(CH ₃) ₂ OOH									
CBS-QB3	-18.70	108.56	42.62	52.69	61.03	67.83	78.14	85.67	97.45
THERM ^b	-18.96	109.75	42.24	52.28	60.81	67.87	78.71	86.90	
*CH ₂ CH(CH ₃)CH ₂ CH ₂ OOH									
CBS-QB3	-6.07	105.82	36.90	44.56	51.41	57.16	66.08	72.64	82.90
THERM ^b	-7.23	104.77	35.75	44.15	51.38	57.51	66.84	73.93	
*CH ₂ C(CH ₃) ₂ CH ₂ CH ₂ OOH									
CBS-QB3	-13.45	110.77	43.28	52.39	60.37	67.04	77.39	85.07	97.13
THERM ^b	-14.23	108.59	41.77	52.12	60.97	68.37	79.32	87.41	

^a Heats of formation in kcal/mol; S^{298} and $C_p(T)$ in cal/mol K. ^b Using Bozzelli's⁷² HBI (hydrogen-bond increment) values. Correction for gauche interactions has been added properly. RCCJC and S are slightly different HBI groups appropriate for secondary alkyl radicals. ^c Calculated using NIST "Structures and Properties" program.⁷⁴

TABLE 8: Thermochemical properties of γ - and β -Hydroperoxyalkyl Radicals (*QOOH) Involved in Oxetane and Oxirane Formation Reactions and Values for the HBI Groups CJCOOH, CCJCOOH, and C₂CJCOOH^a

Species	method	ΔH^{298}	S^{298}	$C_p(T)$						
				300	400	500	600	800	1000	1500
*CH ₂ (CH ₂) ₂ OOH	CBS-QB3	5.32	88.04	24.89	29.95	34.38	38.07	43.72	47.87	54.36
	THERM ^b	4.07	87.23	25.02	30.31	34.81	38.67	44.51	49.11	
	S&P ^c	5.30	87.60	25.00	29.90	34.60	38.00	43.80	47.50	
CH ₃ CH*(CH ₂) ₂ OOH	CBS-QB3	-2.70	98.23	29.54	35.84	41.59	46.47	54.09	59.70	68.39
	THERM; S ^b	-3.51	97.68	29.79	36.29	41.87	47.03	54.99	60.74	
	THERM; RCCJC ^b	-3.51	98.37	29.75	35.85	41.48	46.52	54.39	60.55	
(CH ₃) ₂ C*(CH ₂) ₂ OOH	S&P ^c	-3.00	97.90	30.20	36.30	42.30	46.80	54.30	59.50	
	CBS-QB3	-11.80	105.99	33.55	41.29	48.47	54.63	64.30	71.40	82.34
	THERM ^b	-12.63	103.84	35.74	43.03	49.74	55.76	65.25	72.65	
*CH ₂ CH ₂ OOH	S&P ^c	-11.60	105.20	36.00	43.90	50.80	56.50	65.90	72.30	
	CBS-QB3	11.10	79.04	19.69	23.29	26.39	28.94	32.83	35.68	40.18
	CBS-QB3	-40.06	74.69	19.94	24.05	27.73	30.85	35.69	39.27	44.87
CJCOOH	CBS-QB3	103.26	3.54	-0.25	-0.76	-1.34	-1.91	-2.87	-3.60	-4.69
CJCOOH	THERM ^b	102.87	2.73	-0.66	-1.28	-1.86	-2.35	-3.14	-3.72	
CH ₃ CH*CH ₂ OOH	CBS-QB3	2.66	89.57	24.39	29.22	33.61	37.34	43.17	47.47	54.17
CH ₃ (CH ₂) ₂ OOH	CBS-QB3	-45.21	84.78	25.04	30.61	35.61	39.84	46.44	51.31	58.90
CCJCOOH	CBS-QB3	99.98	4.79	-0.65	-1.40	-2.00	-2.50	-3.27	-3.84	-4.73
(CH ₃) ₂ C*CH ₂ OOH	CBS-QB3	-6.81	96.80	28.29	34.58	40.42	45.45	53.34	59.16	68.13
(CH ₃) ₂ CHCH ₂ OOH	CBS-QB3	-51.91	90.87	31.84	38.74	44.86	50.03	58.08	64.04	73.36
C₂CJCOOH	CBS-QB3	97.20	7.31	-3.54	-4.16	-4.44	-4.58	-4.74	-4.88	-5.23
C ₂ CJCOOH	THERM ^b	96.44	4.59	-0.49	-2.12	-3.22	-3.88	-4.53	-4.87	-5.31

^a Heats of formation in kcal/mol; S^{298} and $C_p(T)$ in cal/mol K. Recommended HBIs are in bold. ^b Using Bozzelli's⁷² HBI (hydrogen-bond increment) values. Correction for gauche interactions has been added properly. RCCJC and S are slightly different HBI groups appropriate for secondary alkyl radicals. ^c Calculated using NIST "Structures and Properties" program.⁷⁴

and oxirane provide the base RSC. 2-Methyl and all dimethyl-substituted oxolanes, oxetanes, and oxiranes require additional stabilizing corrections. However, these corrections seem to be nearly the same, irrespective of the size of the ring. An alkyl

group α to the ether linkage stabilizes it by ~ 1 kcal/mol in methyloxirane, 2-methyloxetane, and 2-methyloxolane, while a dialkyl substitution in any vertex of the ring (as in 2,2-dimethyloxirane, 2,2-dimethyloxetane, 2,2-dimethyloxolane, and

TABLE 9: Thermochemical Properties of Oxolanes (THFs)^a

Species	method	ΔH^{298}	S^{298}	$C_p(T)$						
				300	400	500	600	800	1000	1500
oxolane	NIST	-44.03	72.11	18.45	25.59	32.13	37.64	46.07	52.08	60.97
	CBS-QB3	-44.58	71.09	19.31	26.29	32.72	38.14	46.48	52.46	61.45
	GA (w/o RSC)	-49.26	45.74	24.38	31.30	36.80	41.36	48.76	53.94	
2-Me-oxolane	CBS-QB3	-54.58	80.86	25.43	33.84	41.45	47.86	57.73	64.87	75.71
	GA (w/o RSC)	-58.56	55.92	30.38	38.93	46.00	51.45	60.48	66.78	
3-Me-oxolane	CBS-QB3	-51.82	79.20	25.38	33.67	41.24	47.65	57.57	64.77	75.67
	GA (w/o RSC)	-56.43	53.86	29.61	38.19	45.12	50.85	60.02	66.42	
2,2-diMe-oxolane	CBS-QB3	-64.61	84.56	31.80	41.87	50.73	58.09	69.37	77.56	90.08
	GA (w/o RSC)	-68.16	60.21	36.10	46.32	54.55	61.21	71.89	79.39	
3,3-diMe-oxolane	CBS-QB3	-60.38	84.98	31.63	41.52	50.33	57.71	69.08	77.36	90.00
	GA (w/o RSC)	-64.23	59.05	35.63	46.16	54.71	61.71	72.50	79.90	
Derived Ring Strain Corrections (RSC)										
oxolane	RSC	4.68	25.35	-5.07	-5.01	-4.08	-3.22	-2.28	-1.48	
2-Me-oxolane	RSC	3.98	24.94	-4.95	-5.09	-4.55	-3.59	-2.75	-1.91	
3-Me-oxolane	RSC	4.61	25.34	-4.23	-4.52	-3.88	-3.2	-2.45	-1.65	
2,2-di-Me-oxolane	RSC	3.55	24.35	-4.3	-4.45	-3.82	-3.12	-2.52	-1.83	
3,3-diMe-oxolane	RSC	3.85	25.93	-4.0	-4.64	-4.38	-4.0	-3.42	-2.54	
	av RSC		25.18	-4.51	-4.74	-4.14	-3.43	-2.68	-1.88	

^a Ring strain corrections are derived by taking the difference between the ab initio result and the sum of constituent group values from Benson. Heats of formation in kcal/mol; S^{298} and $C_p(T)$ in cal/mol K.

TABLE 10: Thermochemical Properties of Oxetanes and Oxiranes^a

Species	method	ΔH^{298}	S^{298}	$C_p(T)$						
				300	400	500	600	800	1000	1500
Oxetanes										
oxetane	NIST	-19.25	64.87	14.80	20.07	24.91	28.99	35.24	39.70	46.35
	CBS-QB3	-19.65	65.08	15.10	20.28	25.10	29.16	35.39	39.86	46.59
	GA (w/o RSC)	-44.33	36.32	18.88	24.35	28.55	32.01	37.69	41.60	
2-Me-oxetane	CBS-QB3	-30.67	74.56	21.18	27.86	33.89	38.94	46.70	52.32	60.86
	GA (w/o RSC)	-53.63	46.50	24.88	31.98	37.75	42.10	49.41	54.44	
3-Me-oxetane	CBS-QB3	-27.21	73.96	21.05	27.60	33.58	38.65	46.48	52.16	60.80
	GA (w/o RSC)	-51.50	44.44	24.11	31.24	36.87	41.50	48.95	54.08	
2,2-diMe-oxetane	CBS-QB3	-41.70	79.98	27.67	35.84	43.02	48.99	58.16	64.85	75.15
	GA (w/o RSC)	-63.23	50.79	30.60	39.37	46.30	51.86	60.82	67.05	
Derived Ring Strain Corrections (RSC)										
oxetane	RSC	24.68	28.76	-3.78	-4.07	-3.45	-2.85	-2.30	-1.74	
2-Me-oxetane	RSC	23.55	28.06	-3.70	-4.12	-3.86	-3.16	-2.71	-2.12	
3-Me-oxetane	RSC	24.29	29.52	-3.06	-3.64	-3.29	-2.85	-2.47	-1.92	
2,2-diMe-oxetane	RSC	21.53	29.19	-2.93	-3.53	-3.28	-2.87	-2.66	-2.20	
	av RSC		28.88	-3.37	-3.84	-3.47	-2.93	-2.54	-2.00	
Oxiranes										
oxirane	NIST	-12.58	58.08	11.30	14.74	17.90	20.55	24.57	27.46	31.82
	CBS-QB3	-13.20	57.98	11.39	14.80	17.93	20.55	24.52	27.38	31.74
	GA (w/o RSC)	-39.40	26.90	13.38	17.40	20.30	22.66	26.62	29.26	
Me-oxirane	NIST	-22.63	68.69	17.43	22.23	26.53	30.15	35.77	39.88	46.14
	CBS-QB3	-23.32	68.50	17.33	22.05	26.31	29.90	35.48	39.57	45.88
diMe-oxirane	GA (w/o RSC)	-48.70	37.08	19.38	25.03	29.50	32.75	38.34	42.10	
	CBS-QB3	-33.89	74.30	23.65	29.69	35.02	39.53	46.61	51.86	60.06
	GA (w/o RSC)	-58.30	41.37	25.10	32.42	38.05	42.51	49.75	54.71	
Derived Ring Strain Corrections (RSC)										
oxirane	RSC	26.20	31.08	-1.99	-2.6	-2.37	-2.11	-2.1	-1.88	
1-Me-oxirane	RSC	25.38	31.42	-2.05	-2.98	-3.19	-2.85	-2.86	-2.53	
1,1-diMe-oxirane	RSC	24.41	32.93	-1.45	-2.73	-3.03	-2.98	-3.14	-2.85	
	av RSC		31.81	-1.83	-2.77	-2.86	-2.65	-2.70	-2.42	

^a Ring strain corrections are derived by taking the difference between the ab initio result and the sum of constituent group values from Benson. Heats of formation in kcal/mol; S^{298} and $C_p(T)$ in cal/mol K.

3,3-dimethyloxolane) stabilizes it by ~ 2 kcal/mol. The extra stabilization with dialkyl substitution can be ascribed to compression of the internal angle of the ring, which leads to expansion of the external angle and thereby a relief of steric strain between the alkyl groups.

Determination of Kinetic Parameters. Rate constants $k(T)$ were calculated by standard transition state theory (TST) methods. These $k(T)$ were then fitted to the Arrhenius expressions $k(T) = A \exp(-E_a/RT)$ to obtain the activation energies E_a and frequency factors A . The computed TST $k(T)$ values give nearly linear Arrhenius plots; the fitted $k(T)$ never differs from the TST $k(T)$ by more than 4%. Table 11 lists the fitted

Arrhenius parameters A and E_a of the oxirane, oxetane, and oxolane formation reactions from primary, secondary, and tertiary hydroperoxyalkyl radicals together with literature estimates.

Barrier heights E_a for reactions forming oxetanes or oxiranes from QOOH with any kind of alkyl substitutions can be computed from the Evans–Polanyi relationships presented in Figure 2. For reactions forming oxolanes (THFs), since the barrier height E_a only depends on the nature of radical center, and does not vary with alkyl substituents at positions other than α to the radical center, E_a values can be taken directly from Table 11.

TABLE 11: Computed Rate Parameters (A and E_a) for Cyclic Ether Formation from $\cdot\text{QOOH}$ Radicals, from Fitting Ab Initio $k(T)$ Together with Literature Estimates^a

Method	$\log(A/s^{-1})$	E_a (kcal/mol)	method	$\log(A/s^{-1})$	E_a (kcal/mol)
$\cdot\text{CH}_2\text{CH}_2\text{OOH} \rightarrow \text{oxirane}$			$\cdot\text{CH}_2(\text{CH}_2)_2\text{OOH} \rightarrow \text{oxetane}$		
CBS-QB3	12.60	17.0	CBS-QB3	11.65	21.9
BH&HLYP	12.67	16.7	BH&HLYP	11.89	24.2
BH&HLYP (Chan et al.)	14.0	16.5	BH&HLYP (Chan et al.)	13.1	24.4 (20.8)
Baldwin et al.	12.45	17.11 \pm 1.2	Benson	11.0	15.06
Benson	11.5	14.0	Ranzi	11.3	15.0
Ranzi	11.3	15.0	Curran	10.87	15.25
Curran	11.78	22.0			
$\text{CH}_3\text{CH}\cdot\text{CH}_2\text{OOH} \rightarrow 2\text{-Me-oxirane}$			$\text{CH}_3\text{CH}(\text{CH}_2)_2\text{OOH} \rightarrow 2\text{-Me-oxetane}$		
CBS-QB3	12.14	15.9	CBS-QB3	11.31	19.5
BH&HLYP	12.21	15.2	BH&HLYP	11.51	22.0
BH&HLYP (Chan et al.)	13.6	15.0	BH&HLYP (Chan et al.)	12.7	22.1
Baldwin et al.	12.15	14.89 \pm 1.2			
Ranzi	11.3	15.0	Ranzi	11.3	15.0
Curran	11.78	22.0	Curran	10.87	15.25
$(\text{CH}_3)_2\text{C}\cdot\text{CH}_2\text{OOH} \rightarrow 2,2\text{-diMe-oxirane}$			$(\text{CH}_3)_2\text{C}(\text{CH}_2)_2\text{OOH} \rightarrow 2,2\text{-diMe-oxetane}$		
CBS-QB3	12.49	13.4	CBS-QB3	11.52	17.4
BH&HLYP	12.57	14.2	BH&HLYP	11.52	20.6
BH&HLYP (Chan et al.)	13.9	14.5	BH&HLYP (Chan et al.)	12.5	20.4
Ranzi	11.3	15.0	Ranzi	11.3	15.0
Curran	11.78	22.0	Curran	10.87	15.25
$\cdot\text{CH}_2(\text{CH}_2)_3\text{OOH} \rightarrow \text{oxolane}$			$(\text{CH}_3)_2\text{C}(\text{CH}_2)_3\text{OOH} \rightarrow 2,2\text{-diMe-oxolane}$		
CBS-QB3	10.71	14.8	CBS-QB3	10.41	11.5
BH&HLYP	10.86	17.0	BH&HLYP	10.53	14.7
BH&HLYP (Chan et al.)	12.0	16.4			
Ranzi	11.3	9.5			
Curran	9.97	7.0			
$\text{CH}_3\text{CH}(\text{CH}_2)_3\text{OOH} \rightarrow 2\text{-Me-oxolane}$					
CBS-QB3	10.56	13.0			
BH&HLYP	10.47	15.7			

^a Recommended values are in bold. Uncertainties in recommended values are ~ 2 kcal/mol in E_a .

Barrier heights computed at CBS-QB3 and BH&HLYP differ by ~ 2 kcal/mol; thus, here we estimate ~ 2 kcal/mol uncertainties in the E_a values. The difference in the optimized geometry of the transition state between BH&HLYP and B3LYP does not cause any significant difference in the rotational contribution to the A factor. The major source of uncertainty in the A factors arises from the low frequency vibration of the transition state. Experimentally,^{76,77} the ring puckering vibration of oxetane is found to absorb at 53 cm^{-1} , while the harmonic vibrational frequency obtained for the fully optimized geometry at B3LYP/CBSB7 corresponds to 89 cm^{-1} . One can expect comparable errors ($\pm 36\text{ cm}^{-1}$) in the ring-puckering frequency of the transition state. This corresponds to uncertainties of ± 0.2 in the $\log(A)$ values. In oxolane case, the ring-puckering vibrations obtained in present work at B3LYP/CBSB7 (261 and 581 cm^{-1}) are in good agreement with experiment⁷⁸ (286 and 591 cm^{-1}); thus, we can expect even less uncertainty.

It must be stressed that in computing the A factors, all torsional motions about the single bonds between the non-hydrogen atoms are treated as hindered rotations in the reactant while at the TS the constrained torsions of the cyclic structure are treated as harmonic oscillators (the free methyls and O–OH are treated as hindered rotations). This is a significant improvement compared to the rate estimates presented by Chan et al.,⁴³ wherein all torsional modes were treated as small amplitude vibrations. Consequently, the A values of Chan et al.⁴³ are more than an order of magnitude higher than ours.

The A factor for oxirane formation ($\log A/s^{-1} = 12.60$) is a factor of ~ 9 higher than that for oxetane ($\log A/s^{-1} = 11.65$), which in turn is a factor of ~ 9 higher than for oxolanes ($\log A/s^{-1} = 10.71$). This is consistent with the loss in entropy as one extra rotor is getting frozen with progressive increase of ring size. Curran's mechanism¹⁶ accounts for this entropy loss

by reducing the preexponential factor by a multiple of 8 for every additional frozen rotor.

Although we have derived the general rate estimation rules for the cyclic ether formation from various hydroperoxyalkyl radicals, there are several issues still to be addressed. The cool flame chemistry, as shown schematically in Figure 1, involves significant competition between a variety of pathways, and at high temperature and low pressure this competition will occur under some nonthermal chemically activated energy distribution. Quantitative evaluation of the yield and distribution of cyclic ethers, and more importantly of the chain branching rate (via $\cdot\text{QOOH} + \text{O}_2$), requires accurate estimates of all the competing rates. Unfortunately, the literature rate estimates for most of these competitive pathways do not agree well even to an order of magnitude. For example, the reported rates for intramolecular hydrogen migration between oxygen and carbon centers ($\text{RO}_2 \rightarrow \text{QOOH}$) vary by up to 3 orders of magnitude.^{26,79} We are currently reexamining⁸⁰ these competitive pathways in order to compute reliable $k(T,P)$ for all the channels shown in Figure 1.

Comparison with Experimentally Derived Rate Estimates.

Our calculated upper limit rate constant (1.5 s^{-1}) at 298 K for oxirane formation is consistent with Baldwin's estimation²⁵ (0.8 s^{-1}) derived from gas-phase experiments. The solution phase rate constant from Bloodworth²⁸ at 298 K for oxirane formation from *tert*-butylperoxyalkyl radicals is on the order of $4 \times 10^3\text{ s}^{-1}$. Although rate constants for a particular reaction in the gas phase and in the liquid phase differ frequently by many orders of magnitude owing to solvent effects, Mayo⁸¹ has shown that unimolecular reactions usually have similar rate constants in both gas and liquid phase. So we do not attribute this discrepancy to solvent effects. The difference observed here is largely due to the difference in the O–O bond strength when the leaving group is varied from OH to *t*-BuO. The O–O bond

strength in H₂O₂ (49.3 kcal/mol) is stronger than in RO–OH (Table 3), which in turn is stronger than in RO–OCH₃ (CH₃O–OCH₃ = 39.2 kcal/mol, CH₃CH₂O–OCH₃ = 39.8 kcal/mol, (CH₃)₂CHO–OCH₃ = 41.1 kcal/mol, (CH₃)₃CO–OCH₃ = 41.1 kcal/mol at the CBS-Q level). So, the reaction studied by Bloodworth in solution is expected to be about 6 kcal/mol more exothermic than the simpler hydroperoxyethyl reaction studied by Baldwin; at room temperature this could easily explain the 3 orders of magnitude difference in rates.

Our *A* factor for oxetanes formation from tertiary hydroperoxyalkyl radicals (log *A*/s⁻¹ = 11.52) is in excellent agreement with Mill's²⁹ liquid-phase measurement of 2,2,4,4-tetramethylloxetane formation (log *A*/s⁻¹ = 11.5). Baldwin's²⁶ estimate for the barrier height of formation of 3,3-dimethyloxetane from primary hydroperoxyalkyl radical is lower than the CBS-QB3 prediction (*E*_a = 16.6 and 19.5 kcal/mol, respectively). However, at the temperature range of their study (380–500 °C) our *k*(*T*) is only lower by a factor of 3 than Baldwin's measurement.

Comparison with Previous Theoretical Work. The present barrier-height calculations are largely consistent with those of DeSain et al.⁴⁶ and of Chan et al.,⁴⁹ except that we disagree with DeSain et al.⁴⁶ about the effects of alkyl substituents on the barrier to oxetane formation. Our *A* factors, which carefully include the effects of the hindered rotors in the reactant •QOOH, are significantly lower than those from Chan et al.⁴⁹ Our calculations suggest that the change in *A* factor with ring size is modeled correctly in Curran's isooctane mechanism,¹⁶ though their *A*-factors are all about a factor of 6 smaller than ours.

Our thermochemistry is in good agreement with that of Chen and Bozzelli,⁴⁸ and here we add several new HBI groups and ring-strain corrections. Our finding that the BH&HLYP method used by Chan et al.⁴⁹ systematically overpredicts the exothermicity of the cyclic ether formation provides a caution about their computations, though it appears that their forward reaction barriers are quite good.

Conclusions

Cyclic ether formation reactions from a variety of hydroperoxyalkyl radicals, important in the low-temperature oxidation of hydrocarbons, are analyzed. From our studies on oxolanes formation using a variety of quantum chemistry methods (CBS-Q, CBS-QB3, QCISD, B3LYP, and BH&HLYP), we found that the commonly employed B3LYP functional consistently underestimates the barrier heights of the cyclic ether formation. BH&HLYP barrier heights, on the other hand, are mostly parallel to those of CBS-QB3. However, BH&HLYP thermochemistry is not accurate and it tends to overestimate the reaction exothermicities. CBS-QB3 thermochemistry appears to be accurate, and we used these calculations to derive new thermochemical group values for •QOOH and for cyclic ethers.

A few of the CBS-QB3 barrier heights are inaccurate, due to problems with the higher order extrapolation, denoted Δ*E*(Emp). Correcting ΔΔ*E*(Emp) in those cases by +2.5 kcal/mol results in better agreement between BH&HLYP and CBS-QB3 levels. BH&HLYP barrier heights differ by ~2 kcal/mol from those of CBS-QB3. Experimental results are needed to narrow down this uncertainty.

For a given radical center, the reaction rate to form oxirane is fastest, to form oxolane is next, and oxetane formation is slowest. For a given ring size, the barrier for ring closure follows the order tertiary < secondary < primary, correlating strongly with the overall exothermicity of the reactions. Substitution of alkyl groups adjacent to the OOH group or the radical-bearing carbon has little impact on the barrier height for formation of

oxolanes but affects the barrier for formation of oxetanes and oxiranes, because of release of alkyl strain in the cyclic TS.

Acknowledgment. This work was partially supported by the National Computational Science Alliance under Grants CTS010006N and CTS020009N and utilized the Origin 2000 High-Performance Computing and UniTree Mass Storage systems. We are grateful for financial support from the NSF CAREER program, Alstom Power, Dow Chemical, and the U.S. Department of Energy through grant DE-FG02-98ER14914 and DE-RP-4-01A167057. We thank Dr. Hans-Heinrich Carstensen, Colorado School of Mines, for providing O–O BDEs at the CBS-QB3 level for comparison.

Supporting Information Available: The isodesmic reactions, literature heat of formation values, and BH&HLYP/6-311G** enthalpies (298 K) used in calculating heats of formation of •OH, RO• and ROOH are given in Table A. Individual component energies, viz., *E*(SCF), Δ*E*(MP2), Δ*E*(MP34), Δ*E*(CCSD), Δ*E*(CBS), Δ*E*(Int), Δ*E*(Emp), and Δ*E*(ZPE) (in hartrees) of the absolute CBS-QB3 energies of the reactants and transition states are given in Table B. The difference in the component energies between the reactant and the corresponding transition states, viz., ΔΔ*E*(components) are given in kcal/mol. The B3LYP/CBSB7-optimized Cartesian coordinates (in Å) and unscaled harmonic vibrational frequencies of the transition structures involved in the reactions forming oxolanes, oxetanes, and oxiranes are tabulated in Tables C and D, respectively. The BH&HLYP/6-311G**-optimized Cartesian coordinates (in Å) and unscaled harmonic vibrational frequencies of the transition structures involved in reactions forming oxetanes and oxiranes from methyl substituted (α to OOH and β to radical center) QOOH are given in Tables E and F. This material is available free of charge via the Internet at <http://pubs.acs.org>.

References and Notes

- (1) Aoyama, T.; Hattori, Y.; Mizuta, H.; Sato, Y. *SAE Paper No. 960081* 1996.
- (2) Pitz, W. J.; Westbrook, C. K. *Combust. Flame* **1986**, *63*, 113.
- (3) Ranzi, E.; Sogaro, A.; Gaffuri, P.; Pennati, G.; Westbrook, C. K.; Pitz, W. J. *Combust. Flame* **1994**, *99*, 201.
- (4) Griffiths, J. F. *Prog. Energy Combust. Sci.* **1995**, *21*, 25.
- (5) Curran, H. J.; Gaffuri, P.; Pitz, W. J.; Westbrook, C. K. *Combust. Flame* **1998**, *114*, 149.
- (6) Warth, V.; Stef, N.; Glaude, P. A.; Battin-Leclerc, F.; Scacchi, G.; Come, G. M. *Combust. Flame* **1998**, *114*, 81.
- (7) Walker, R. W. *Research in Chemical Kinetics*; Elsevier: Amsterdam, 1995; Vol. 3.
- (8) Walker, R. W.; Morley, C. *Low-Temperature Combustion and Autoignition*; Elsevier: Amsterdam, 1997.
- (9) Robertson, S. H.; Seakins, P. W.; Pilling, M. J. *Low-Temperature Combustion and Autoignition*; Elsevier: Amsterdam, 1997.
- (10) Pollard, R. T. *Gas Phase Combustion*; Elsevier: Amsterdam, 1977.
- (11) Jones, J. H.; Fenske, M. R. *Ind. Eng. Chem.* **1959**, *51*, 262.
- (12) Ciajolo, A.; D'Anna, A. *Combust. Flame* **1998**, *112*, 617.
- (13) Dagaut, P.; Reuillon, M.; Cathonnet, M. *Combust. Flame* **1995**, *101*, 132.
- (14) Minetti, R.; Carlier, M.; Ribaucour, M.; Therssen, E.; Sochet, L. R. *Combust. Flame* **1995**, *102*, 298.
- (15) Minetti, R.; Carlier, M.; Ribaucour, M.; Therssen, E.; Sochet, L. R. *Proc. Combust. Inst.* **1996**, *26*, 747.
- (16) Curran, H. J.; Gaffuri, P.; Pitz, W. J.; Westbrook, C. K. *Combust. Flame* **2002**, *129*, 253.
- (17) Ranzi, E.; Gaffuri, P.; Faravelli, T.; Dagaut, P. *Combust. Flame* **1995**, *103*, 91.
- (18) Ranzi, E.; Faravelli, T.; Gaffuri, P.; Sogaro, A. *Combust. Flame* **1997**, *108*, 24.
- (19) Glaude, P. A.; Warth, V.; Fournet, R.; Battin-Leclerc, F.; Come, G. M.; Scacchi, G. *Bull. Soc. Chim. Belg.* **1997**, *106*, 343.
- (20) Wong, B. M.; Matheu, D. M.; Green, W. H., Jr. *J. Phys. Chem. A* Submitted.

- (21) Rienstra-Kiracofe, J. C.; Allen, W. D.; Schaefer, H. F., III *J. Phys. Chem. A* **2000**, *104*, 9823.
- (22) Benson, S. W. *J. Am. Chem. Soc.* **1965**, *87*, 972.
- (23) Benson, S. W. *The Mechanism of Pyrolysis, Oxidation and Burning of Organic Compounds*; Nat. Bur. Stand. Special Publication 357; U.S. Department of Commerce: Washington, DC, 1972.
- (24) Fish, A. *Organic Peroxides*; Wiley: New York, 1970; Vol. 1.
- (25) Baldwin, R. R.; Dean, C. E.; Walker, R. W. *J. Chem. Soc., Faraday Trans. 2* **1986**, *82*, 1445.
- (26) Baldwin, R. R.; Dean, C. E.; Walker, R. W. *J. Chem. Soc., Faraday Trans. 1* **1982**, *78*, 1615.
- (27) Bloodworth, A. J.; Davies, A. G.; Griffin, I. M.; Muggleton, B.; Roberts, B. P. *J. Am. Chem. Soc.* **1974**, *96*, 7599.
- (28) Bloodworth, A. J.; Courtneidge, J. L.; Davies, A. G. *J. Chem. Soc., Perkin Trans. 2* **1984**, *80*, 523.
- (29) Mill, T. *Proc. Combust. Inst.* **1971**, *13*, 237.
- (30) DeSain, J. D.; Clifford, E. P.; Taatjes, C. A. *J. Phys. Chem. A* **2001**, *105*, 3205.
- (31) DeSain, J. D.; Taatjes, C. A. *J. Phys. Chem. A* **2001**, *105*, 6646.
- (32) Clifford, E. P.; Farrell, J. T.; DeSain, J. D.; Taatjes, C. A. *J. Phys. Chem. A* **2000**, *104*, 11549.
- (33) Kaiser, E. W.; Lorkovic, I. M.; Wallington, T. J. *J. Phys. Chem.* **1990**, *94*, 3352.
- (34) Kaiser, E. W.; Wallington, T. J.; Andino, J. M. *Chem. Phys. Lett.* **1990**, *168*, 309.
- (35) Kaiser, E. W. *J. Phys. Chem.* **1995**, *99*, 707.
- (36) Kaiser, E. W.; Rimai, L.; Wallington, T. J. *J. Phys. Chem.* **1989**, *93*, 3, 4094.
- (37) Kaiser, E. W.; Wallington, T. J. *J. Phys. Chem.* **1996**, *100*, 18770.
- (38) Kaiser, E. W. *J. Phys. Chem. A* **1998**, *102*, 5903.
- (39) Kaiser, E. W. *J. Phys. Chem. A* **2002**, *106*, 1256.
- (40) Bozzelli, J. W.; Dean, A. M. *J. Phys. Chem.* **1990**, *94*, 3313.
- (41) Wagner, A. F.; Slagle, I. R.; Sarzynski, D.; Gutman, D. *J. Phys. Chem.* **1990**, *94*, 1858.
- (42) Ignatyev, I. S.; Xie, Y.; Allen, W. D.; Schaefer, H. F. *J. Chem. Phys.* **1997**, *107*, 141.
- (43) Miller, J. A.; Klippenstein, S. J. *Int. J. Chem. Kinet.* **2001**, *33*, 654.
- (44) Chen, C. J.; Bozzelli, J. W. *J. Phys. Chem. A* **2000**, *104*, 4997.
- (45) Lay, T. H.; Bozzelli, J. W. *J. Phys. Chem. A* **1997**, *101*, 9505.
- (46) DeSain, J. D.; Taatjes, C. A.; Miller, J. A.; Klippenstein, S. J.; Hahn, D. K. *Faraday Discussions* **2001**, *119*, 101.
- (47) Jungkamp, T. P. W.; Smith, J. N.; Seinfeld, J. H. *J. Phys. Chem. A* **1997**, *101*, 4392.
- (48) Chen, C. J.; Bozzelli, J. W. *J. Phys. Chem. A* **1999**, *103*, 9731.
- (49) Chan, W. T.; Hamilton, I. P.; Pritchard, H. O. *Phys. Chem. Chem. Phys.* **1999**, *1*, 3715.
- (50) Sumathi, R.; Green, W. H., Jr. *Theor. Chem. Acc.* **2002**, *108*, 187.
- (51) Sumathi, R.; Carstensen, H.-H.; Green, W. H., Jr. *J. Phys. Chem. A* **2001**, *105*, 6910.
- (52) Sumathi, R.; Carstensen, H.-H.; Green, W. H., Jr. *J. Phys. Chem. A* **2001**, *105*, 8969.
- (53) Sumathi, R.; Carstensen, H.-H.; Green, W. H., Jr. *J. Phys. Chem. A* **2002**, *106*, 5474.
- (54) Sumathi, R.; Green, W. H., Jr. *Phys. Chem. Chem. Phys.* Submitted.
- (55) Frisch, M. J.; Trucks, G. W.; Schlegel, H. B.; Scuseria, G. E.; Robb, M. A.; Cheeseman, J. R.; Zakrzewski, V. G.; Montgomery, J. A., Jr.; Stratmann, R. E.; Burant, J. C.; Dapprich, S.; Millam, J. M.; Daniels, A. D.; Kudin, K. N.; Strain, M. C.; Farkas, O.; Tomasi, J.; Barone, V.; Cossi, M.; Cammi, R.; Mennucci, B.; Pomelli, C.; Adamo, C.; Clifford, S.; Ochterski, J. W.; Petersson, G. A.; Ayala, P. Y.; Cui, Q.; Morokuma, K.; Malick, D. K.; Rabuck, A. D.; Raghavachari, K.; Foresman, J. B.; Cioslowski, J.; Ortiz, J. V.; Baboul, A. G.; Stefanov, B. B.; Liu, G.; Liashenko, A.; Piskorz, P.; Komaromi, I.; Gomperts, R.; Martin, A. L.; Fox, D. J.; Keith, T.; Al-Laham, M. A.; Peng, C. Y.; Nanayakkara, A.; Challacombe, M.; Gill, P. M. W.; Johnson, B.; Chen, W.; Wong, M. W.; Andres, J. L.; Gonzalez, C.; Head-Gordon, M.; Replogle, E. S.; Pople, J. A. *Gaussian 98*, Revision A.9; Gaussian Inc.: Pittsburgh, PA., 1998.
- (56) Montgomery, J. A., Jr.; Ochterski, J. W.; Petersson, G. A. *J. Chem. Phys.* **1994**, *101*, 5900.
- (57) Ochterski, J. W.; Petersson, G. A.; Montgomery, J. A., Jr. *J. Chem. Phys.* **1996**, *104*, 2598.
- (58) Sumathi, R.; Green, W. H., Jr. *J. Phys. Chem. A* **2002**, *106*, 11141.
- (59) Scott, A. P.; Radom, L. *J. Phys. Chem.* **1996**, *100*, 16502.
- (60) Nicolaides, A.; Rauk, A.; Glukhovtsev, M. N.; Radom, L. *J. Phys. Chem.* **1996**, *100*, 17460.
- (61) Petersson, G. A.; Malick, D. K.; Wilson, W. G.; Ochterski, J. W.; Montgomery, J. A., Jr.; Frisch, M. J. *J. Chem. Phys.* **1998**, *109*, 10570.
- (62) Parkinson, C. J.; Mayer, P. M.; Radom, L. *Theor. Chem. Acc.* **1999**, *102*, 92.
- (63) Brinck, T.; Lee, H.-N.; Jonsson, M. *J. Phys. Chem. A* **1999**, *103*, 7094.
- (64) Green, W. H., Jr. *Int. J. Quantum Chem.* **1994**, *52*, 837.
- (65) <http://webbook.nist.gov>. National Institute of Standard and Technology, 2002; Vol. 2002.
- (66) Curtiss, L. A.; Redfern, P. C.; Raghavachari, K.; Pople, J. A. *J. Chem. Phys.* **2001**, *114*, 108.
- (67) Zhang, Q.; Bell, R.; Truong, T. N. *J. Phys. Chem.* **1995**, *99*, 592.
- (68) Durant, J. L. *Chem. Phys. Lett.* **1996**, *256*, 595.
- (69) Lynch, B. J.; Truhlar, D. G. *J. Phys. Chem. A* **2001**, *105*, 2936.
- (70) Pipek, J.; Mezey, P. G. *J. Chem. Phys.* **1989**, *90*, 4916.
- (71) Montgomery, J. A., Jr.; Frisch, M. J.; Ochterski, J. W.; Petersson, G. A. *J. Chem. Phys.* **2000**, *112*, 6532.
- (72) Lay, T. H.; Bozzelli, J. W.; Dean, A. M.; Ritter, E. R. *J. Phys. Chem.* **1995**, *99*, 14514.
- (73) Smith, B. J.; Radom, L. *J. Phys. Chem. A* **1998**, *102*, 10787.
- (74) NIST. Standard Reference Database 19A. In *Structure and Properties*, 2.02 ed.; NIST: Gaithersburg, MD, 1994.
- (75) Cohen, N. J. *Phys. Chem. Ref. Data* **1996**, *25*, 1411.
- (76) Moruzzi, G.; Kunzmann, M.; Winnewisser, B. P.; Winnewisser, M. 16th International Colloquium on High-Resolution Molecular Spectroscopy, 1999, Dijon, France.
- (77) Jokisaari, J.; Kauppinen, J. *J. Chem. Phys.* **1973**, *59*, 2260.
- (78) Cadioli, B.; Gallinella, E. *J. Phys. Chem.* **1993**, *97*, 7844.
- (79) Chan, W. T.; Hamilton, I. P.; Pritchard, H. O. *J. Chem. Soc., Faraday Trans.* **1998**, *94*, 2303.
- (80) Sumathi, R.; Green, W. H., Jr. Manuscript in preparation.
- (81) Mayo, F. R. *J. Am. Chem. Soc.* **1967**, *89*, 2654.